



## Preparation, Characterization and Biological Studies of New Tetra-Dentate N4 Schiff Base Derived from Malonic Acid Dihydrazide with Mn<sup>+2</sup> and Co<sup>+2</sup> Complexes

Rehab Ghalib Hammuda<sup>1\*</sup>   and Naser Dheyaa Shaalan<sup>2</sup>  

<sup>1,2</sup> Department of Chemistry, College of Sciences for Women University of Baghdad, Baghdad, Iraq.

\*Corresponding Author.

Received: 2 March 2023

Accepted: 30 March 2023

Published: 20 April 2024

[doi.org/10.30526/37.2.3304](https://doi.org/10.30526/37.2.3304)

### Abstract

New complexes were synthesized from a newly prepared Schiff base ligand (L<sub>2</sub>) derived from malonic acid dihydrazide and 2-pyridine carboxaldehyde. The <sup>1</sup>H-NMR and <sup>13</sup>C-NMR spectra demonstrated all the needed peaks to prove the chemical structure of the synthesized ligand (L<sub>2</sub>). Utilizing mass spectroscopy, the molecular ion peak was found at m/e 310, confirming the formula weight for L<sub>2</sub>, which matches the estimated m+ value (310.12). Accordingly, its Mn (II) and Co (II) complexes were trained using glacial acetic acid as a catalyst. These compounds were characterized by FT-IR, UV-Vis, C.H.N., chloride-containing, molar conductance, magnetic susceptibility, and atomic absorption. The characterization results gave complexes hexadentate coordination geometry for each cobalt and manganese complex. Schiff base ligand acted as tetradentate with a good yield. The biological activities of the new compounds were valued against two Gram-positive (*Staphylococcus aureus* and *Bacillus subtilis*), two Gram-negative (*Escherichia coli* and *Pseudomonas aeruginosa*), and candida fungi; hence, their results were good in inhibition.

**Keywords:** Biological activities, *Candida fungi*, inhibition, 2-pyridine carboxaldehyde, Schiff base complexes.

### 1. Introduction

Schiff's bases are widely used in coordination chemistry because of their high coordination number and ability to form complexes with a wide variety of metal ions, including those of transition metal. In this study, primary amines and active carbonyl groups can condense to form Schiff's bases; two different mechanisms can make an imine. The amine nitrogen's nucleophilic activity first attacks the electrophilic carbonyl carbon of aldehydes or ketones as a nucleophile. The nitrogen deprotonates in the subsequent stage, and the electrons from this N-H bond push the oxygen away from the carbon, leaving a compound with a C=N double bond (an imine), which displaces a water molecule.



Derivatives of hydrazone are well-recognized for a variety of biological functions. Numerous hydrazones have been used as antibacterial medications, which are often employed for the treatment of various biological activities. Malonic acid hydrazide and 2-pyridine carboxaldehyde compounds are significant classes of polydentate ligands in coordination chemistry and have many uses in multiple fields [1]. In addition, the presence of an imine group is essential for understanding how transformation and racemization reactions occur in biological systems [2]. Transition-metal complexes of hydrazone and its derivatives have garnered significant attention due to their diverse applications, such as antibacterial, anti-tubercular, carbonic anhydrase inhibition, and anti-inflammatory properties. These complexes have been extensively studied, reflecting their potential health-related applications. Discoveries in the field of bioinorganic chemistry have heightened interest in macrocyclic complexes containing oxygen and nitrogen atoms [5, 6]. This study describes the synthesis of a novel Schiff base [L<sub>2</sub>] and uses it as a ligand to provide sites that are potential donors and form complexes with Mn (II) and Co (II). The ligand [L<sub>2</sub>] and its complexes have been fully characterized.

## 2. Materials and Methods

### 2.1 Materials

The chemicals used in this study diethyl malonate (Sigma Aldrich 99%), hydrazine monohydrate (99%, 2-pyridine carboxaldehyde (Sigma Aldrich 98%), Absolute Ethanol (B.D.H, 99%), CoCl<sub>2</sub>.6H<sub>2</sub>O 99% and MnCl<sub>2</sub>.4H<sub>2</sub>O 99% were provided from BDH.

The University of Tehran's labs measured the nitrogen and carbon-hydrogen (CHN) contents. Shimadzu FT-IR-8100 spectrometers were used to record FT-IR spectra at the labs of the University of Baghdad's College of Science. The University of Tehran's laboratories were also used to determine the ligand's <sup>1</sup>H NMR and <sup>13</sup>C NMR spectra using d<sub>6</sub>-DMSO as a solvent and TMS as an internal standard on a Bruker 400 MHz. A UV-1650 PC Shimadzu spectrophotometer was used to measure the electronic spectra at a temperature of 25 °C. The experiments were conducted in the labs of the College of Sciences for Women at the University of Baghdad, utilizing complexes with a concentration of (10<sup>-3</sup> M) in absolute DMF.

A Philips PW-digital conductivity meter was used to test the electrical conductivity of the complexes in a (1 × 10<sup>-3</sup> M) solution of the samples in DMF at room temperature. The measurements were performed at the University of Baghdad's College of Science for Women. At Al Mustansiriya University, all magnetic susceptibility values for the solid state were likewise obtained using the Gouy balance. By using a GCMS-QP2010 PLUS DI analysis Shimadzu, Japan, spectrometer in the University of Samarra's lab, the molecular weight of the produced ligand was ascertained. Additionally, all melting point values were recorded using the Gallen Kamp melting equipment at the College of Science for Women, University of Baghdad.

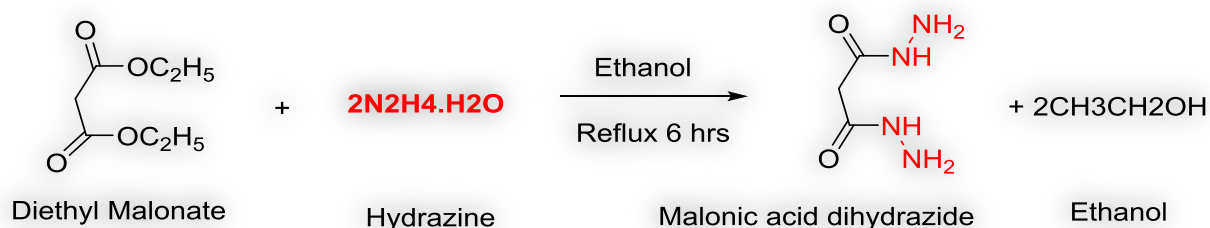
### 2.2 Synthesis

#### 2.2.1 Synthesis of ligand (L<sub>2</sub>)

**Step I:** Including the preparation of malonic acid dihydrazide, the synthesis method is described below:

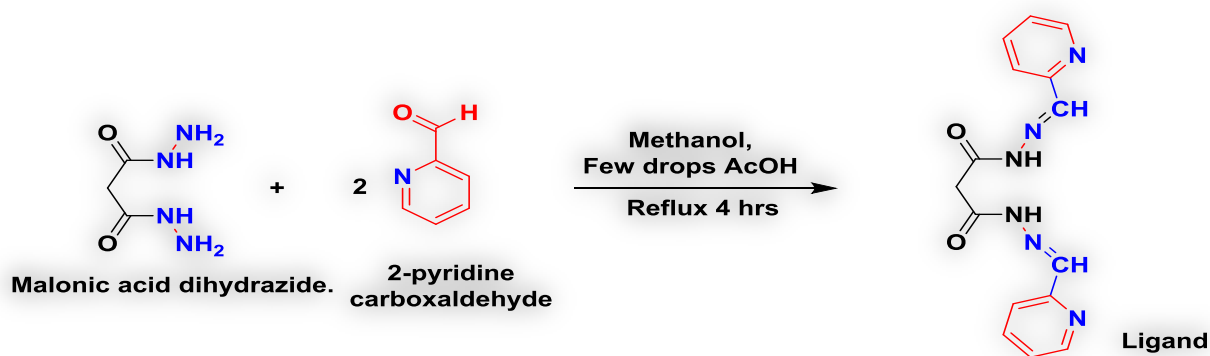
A solution of (10 g, 0.062 mol) of diethyl malonate was stirred in a round bottom flask in 10 mL ethanol at room temperature. Then (6.2 g, 0.124 mol) of aqueous hydrazine was added dropwise with continuous stirring, then refluxed for 6 hrs. When the reaction was stopped and cooled down to room temperature the white precipitate was filtered and washed with methanol

and then dry ether. White precipitate recrystallized from absolute ethanol gave a very good yield of 80 % (7.1g), m.p 159 °C. **Scheme 1** represents the preparation of Malonic acid dihydrazid.



**Scheme 1.** Steps of preparation of malonic acid dihydrazide.

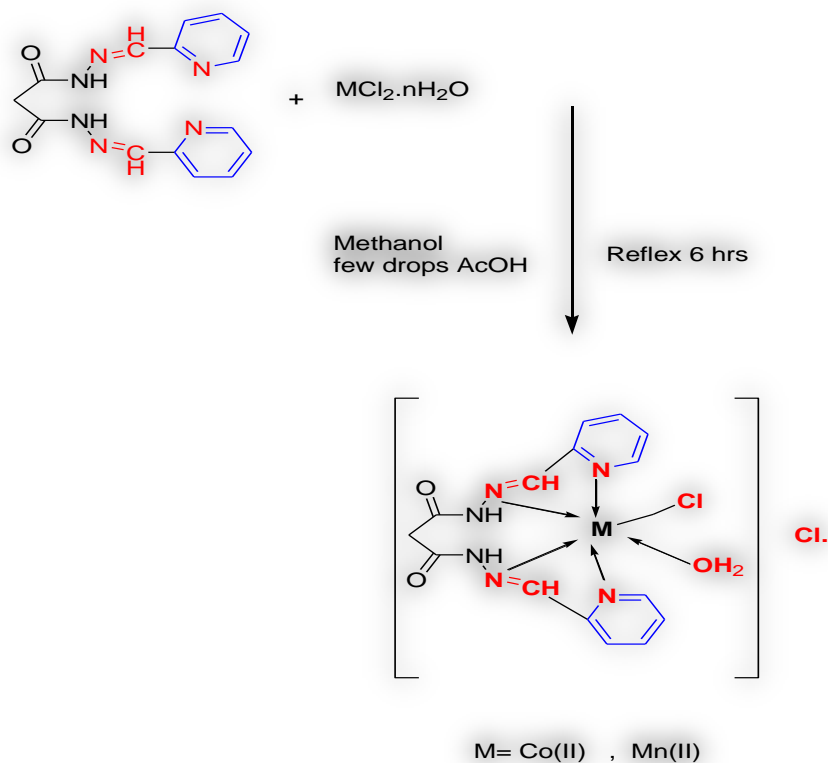
**Step II:** A methanolic solution (15 mL) of 2-pyridine carboxaldehyde (1.62 g, 0.015 mol) was added to a mixture containing a methanolic solution (15 mL) of malonic acid dihydrazid (1.0 g, 0.007 mol) under nitrogen gas, then adding 1-2 drops of glacial acetic acid, as shown in **Scheme 2**. The resulting mixture was refluxed for 4 hours with stirring. After that, the mixture was cooled down to room temperature, and white crystals were formed, filtered, washed, and then re-crystallized from ethanol. The product was dried over anhydrous CaCl<sub>2</sub> under a vacuum to yield a pure product of 86% (2.0 g), m.p. 214–216 °C.



**Scheme 2.** Synthesis of Schiff bases ligand (L<sub>2</sub>).

### 2.2.2 General procedure to synthesis metal ions Mn<sup>2+</sup>, and Co<sup>2+</sup> complexes

The prepared ligand (L<sub>2</sub>) (0.2 g, 0.6 mmol) was dissolved in methanol (10 mL) with stirring. Metal chloride hydrate (0.1 g, 0.6 mmol) was dissolved in methanol (10 mL) and added to the ligand solution, as shown in **Scheme 3**. The mixture was heated under reflux for 5 hours; during this period, the colour of the solid changed to dark green. The green precipitate was then collected by filtration, washed with methanol, and dried at room temperature for 48 hrs to get 78–81%, see **Table 1**.



**Scheme 3.** Synthesis of Schiff base Metal Complexes.

### 3. Results and Discussion

The tetradentate ligand [L<sub>2</sub>] was produced in high yield by the reaction of one mole of malonic acid dihydrazide and two moles of 2-pyridine carboxaldehyde. **Table 1** summarizes the physical properties and micro-elemental analysis of the prepared ligand and its metal complexes. The results are quite related to the suggested structural formula. The formation of ligands and complexes has been demonstrated by the close match between the calculated and observed values of the elemental analysis.

**Table 1.** The physical properties of the prepared compounds.

Formula	% Theoretical (Experimental)								
	Color	m.p. °C	M.wt	%Yield	%C	%H	%N	%Cl	%M
L <sub>2</sub>	White	214-216	310.32	86%	58.06	4.55	27.8		
C <sub>15</sub> H <sub>14</sub> N <sub>6</sub> O <sub>2</sub>					(57.11)	(5.23)	(26.91)		
[MnL <sub>2</sub> Cl(H <sub>2</sub> O)]Cl·H <sub>2</sub> O	Yellow	235-243 d	472.19	78%	38.15	3.84	17.80	15.02	11.63
C <sub>15</sub> H <sub>18</sub> Cl <sub>2</sub> Mn N <sub>6</sub> O <sub>4</sub>					(39.31)	(3.21)	(18.11)	(14.63)	(11.01)
[CoL <sub>2</sub> Cl(H <sub>2</sub> O)]Cl	Dark - green	225-229	458.17	81%	39.32	3.52	(18.34)	(15.48)	(12.86)
C <sub>15</sub> H <sub>16</sub> Cl <sub>2</sub> CoN <sub>6</sub> O <sub>3</sub>					(40.20)	(4.10)	(17.97)	(15.74)	(12.59)

d= decompose

### 3.1 The UV-visible spectroscopy

#### 3.1.1 The UV-visible for the ligand and its complexes

The electronic spectra of the ligand and ligand complexes were recorded in their solution in DMF in the range of (200-1100) nm, as in **Table 2** and **Figures 1–3**. The electronic spectrum of the ligand shows intense absorption at 314-331 that belongs to ( $\pi \rightarrow \pi^*$ ) and ( $n \rightarrow \pi^*$ ), respectively [7-12]. **Table 2** summarizes the conductivity data, which show electrolyte behavior. The electronic spectrum of Co (II) complex showed three peaks at 368, 607, and 673, C.T,  $4T1g(F) \rightarrow 4T1g(P)$ ,  $4T1g(F) \rightarrow 4A2g$ , respectively [13–15], and the electronic spectrum of Mn (II) showed three peaks at 228, 289, and 347 nm assigned to ( $\pi \rightarrow \pi^*$ ), ( $n \rightarrow \pi^*$ ) and  $6A1g \rightarrow 4T1g(G)$  with charge transfer, respectively [16, 17], suggesting all the complexes are octahedral geometry (11–14). All the data for the electronic spectra are listed in **Table 3**.

**Table 2.** Magnetic moments, and molar conductivity for Schiff base ligand and its complexes.

Complexes	$\mu_{eff}^{(cal)}$ (B.M)	Magnetic moment	Molar Cond. $\text{Ohm}^{-1} \text{cm}^2 \cdot \text{mol}^{-1}$	Type
$[\text{MnL}_2\text{Cl}(\text{H}_2\text{O})] \text{Cl} \cdot \text{H}_2\text{O}$	6.37	Paramagnetic High spin	75	Electrolyte
$[\text{CoL}_2\text{Cl}(\text{H}_2\text{O})]\text{Cl}$	4.52	Paramagnetic High spin	90	Electrolyte

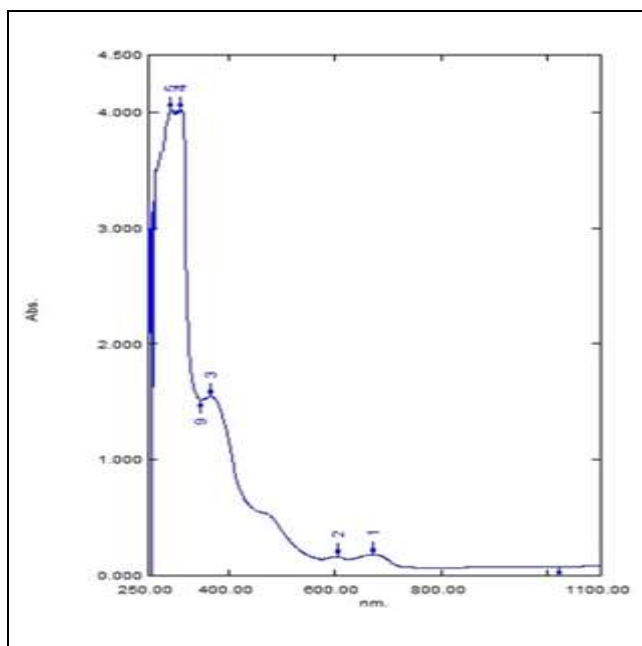


**Figure 2.** The UV-spectrum of Co  $L_2$  complex

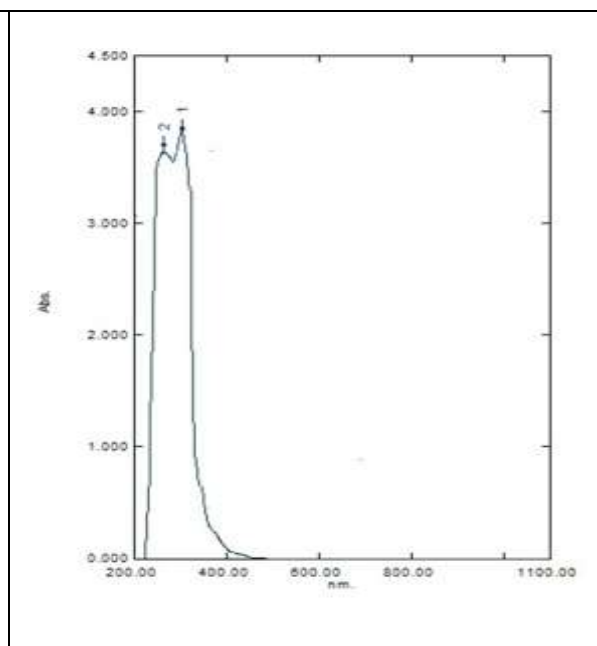


**Figure 1.** The UV-spectrum of  $L_2$

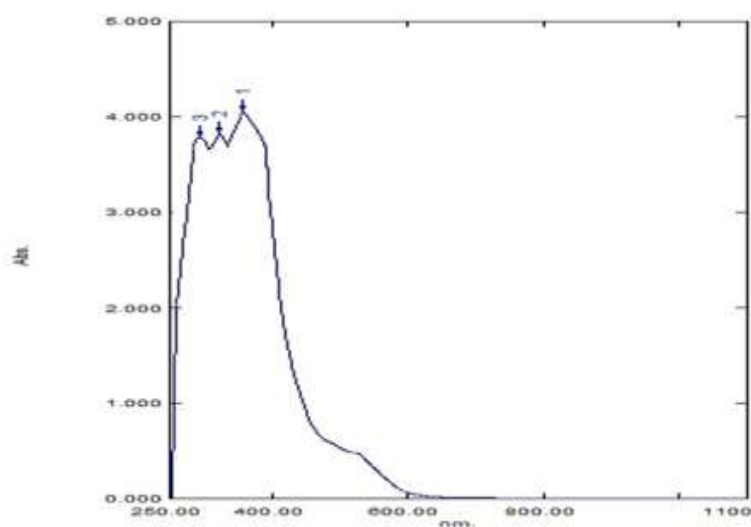


Figure 3. The UV- spectrum of Mn L<sub>2</sub> complex.

Table 3. Electronic spectra, for Schiff base ligand and its complexes.

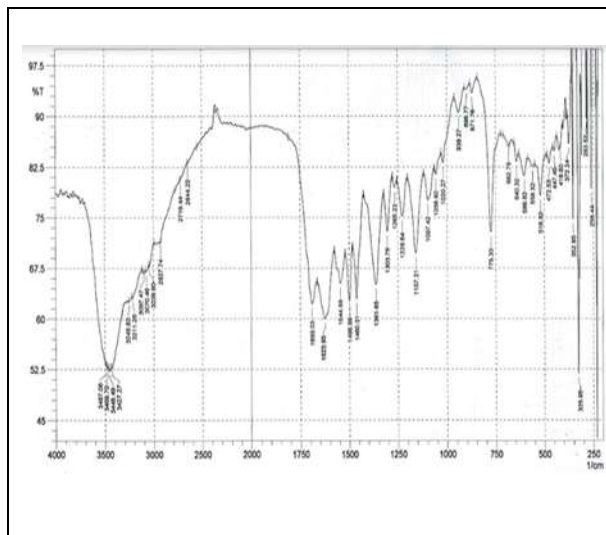
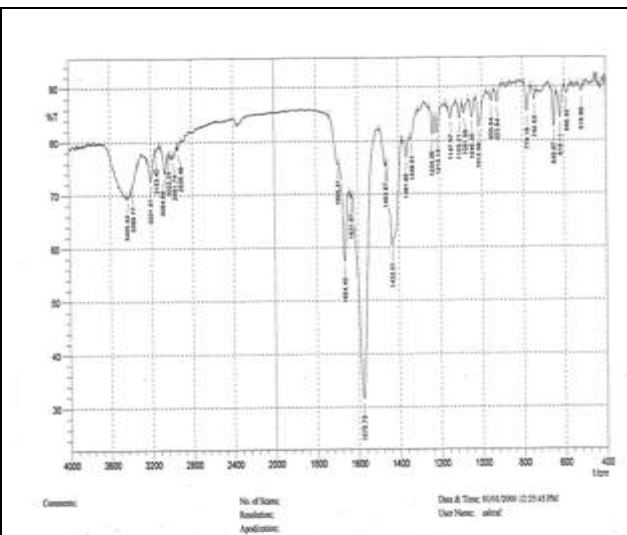
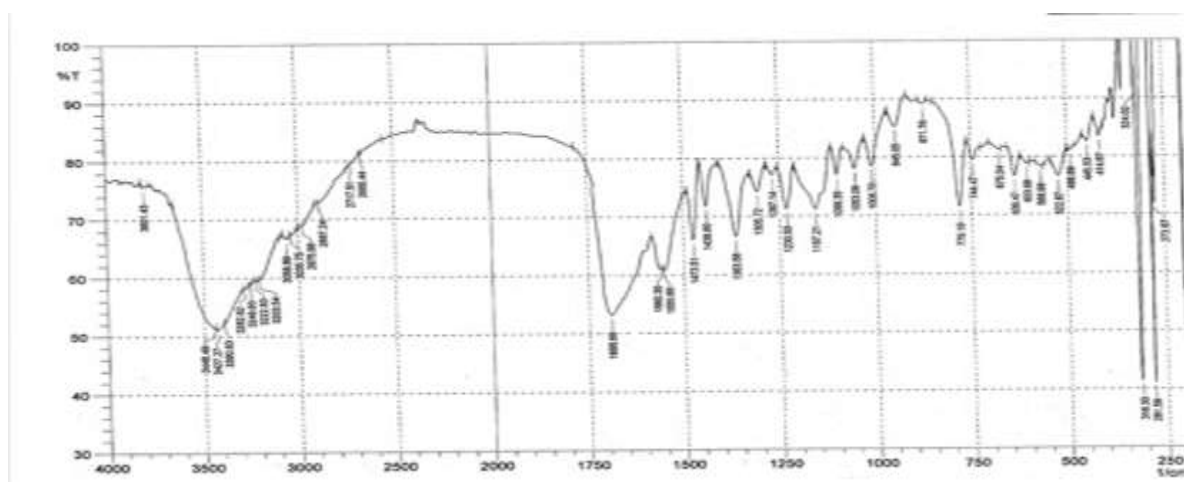
Compound	Electronic arrangement	State	$\lambda_{\max}$ (nm)	Absorption bands $\text{cm}^{-1}$	Assignments
C <sub>15</sub> H <sub>14</sub> N <sub>6</sub> O <sub>2</sub>	-	-	314	31847.1	$\pi \rightarrow \pi^*$
			331	30211.4	$n \rightarrow \pi^*$
[MnL <sub>2</sub> Cl(H <sub>2</sub> O)]Cl.H <sub>2</sub> O	d <sup>5</sup>	<sup>6</sup> S	228	4385.96	$\pi \rightarrow \pi^*$
			289	346020	$n \rightarrow \pi^*$
			347	28818.4	<sup>6</sup> A <sub>1g</sub> → <sup>4</sup> T <sub>1g</sub> (G) with C.T
[CoL <sub>2</sub> Cl(H <sub>2</sub> O)]Cl	d <sup>7</sup>	<sup>4</sup> F, <sup>4</sup> P	673	27173.9	<sup>4</sup> T <sub>1g</sub> (F) → <sup>4</sup> A <sub>2g</sub> (F)
			607	16474.4	<sup>4</sup> T <sub>1g</sub> (F) → <sup>4</sup> T <sub>1g</sub> (P)
			368	14858.8	C.T

### 3.2 Infrared spectral studies of ligand and the complexes

The tetradentate Schiff base L<sub>2</sub> displays a sharp band at 3014  $\text{cm}^{-1}$  and 3431  $\text{cm}^{-1}$  assigned to  $\nu(\text{C-H})$  and  $\nu(\text{N-H})$ , respectively [18]. A strong band appeared at 1664  $\text{cm}^{-1}$  assigned to the stretching band of the azomethine group, as observed in **Table 4** and **Figure 4**. The coordination of the metal ions to the nitrogen azomethine leads to a shift-down in the frequency of  $\nu(\text{C=N})$  value due to the decreases in the electron density on the azomethine after donating electrons of nitrogen to the partially filled d-orbitals of the metal ions (II) [19, 20]. The IR spectra of the complexes exhibit characteristic bands around (1560-1608)  $\text{cm}^{-1}$ , showing that the metal ions coordinate with L<sub>2</sub> via the azomethine nitrogen atom [21]. The stretching vibrations of the nitrogen in the pyridine group cause a prominent band at 1413-1363  $\text{cm}^{-1}$ . New stretching modes were observed in the far-infrared spectra of the complexes that didn't exist in the spectrum of L at (445-462)  $\text{cm}^{-1}$  and (347-352)  $\text{cm}^{-1}$  and (518-522)  $\text{cm}^{-1}$ , which are attributed to (M-N), (M-Cl) and (M-O) as evidence on the formation bonds between the metal ions (II) and the nitrogen azomethine chloride and oxygen, respectively, as observed in **Figures 5** and **6** [22-24].

**Table 4.** Electronic spectra, for Schiff base L<sub>2</sub> and its complexes.

Compound	N-H stretch 2 bands	H <sub>2</sub> O Coord	CH Ar	CH Aph	C=O	C=N	N-H in plane	C-N	N-H out of plane	H <sub>2</sub> O Coord	M- O	M- N	M- Cl
C <sub>15</sub> H <sub>14</sub> N <sub>6</sub> O <sub>2</sub>	3431	---	3014	2879	1693	1664	1556	1413	642	---	---	---	---
[MnL <sub>2</sub> Cl(H <sub>2</sub> O)]Cl.H <sub>2</sub> O	3427	3390	3035	2975	1696	1560	1473	1363	636	779- 568	522	445	316
[CoL <sub>2</sub> Cl(H <sub>2</sub> O)]Cl	3427	3249	3039	2972	1693	1623	1496	1361	640	775- 559	518	447	352

**Figure 5.** The FTIR-spectrum of CoL<sub>2</sub> complex.**Figure 4.** The FTIR-spectrum of L<sub>2</sub>.**Figure 6.** The FTIR-Spectrum of MnL<sub>2</sub> complex.

### 3.3 Proton nuclear magnetic resonance spectroscopy (<sup>1</sup>H-NMR)

The chemical environment of organic molecules can be determined using nuclear magnetic resonance spectroscopy. Using tetramethylsilane (TMS) as the internal reference standard, the <sup>1</sup>H-NMR of the ligand (L<sub>2</sub>) in dimethyl sulfoxide (DMSO-d<sub>6</sub>) is shown in **Figure 7**. The produced ligand's chemical structure was confirmed by the <sup>1</sup>H-NMR, which showed all the required peaks (L<sub>2</sub>). The ligand displayed a singlet peak at a chemical shift of 3.07 ppm, which belongs to the aliphatic CH<sub>2</sub> group. This peak has shifted to a higher chemical shift because it is next to two carbonyl groups, which cause the de-shielding of electrons around the corresponding protons. While the proton of the azomethine group (HC=N) shows a singlet peak at a chemical

shift of 7.94 ppm, the four protons of the heteroaromatic unit show multiplet peaks at regions between 7.5 ppm and 7.8 ppm, except one proton was shifted to a higher chemical shift, showing a nice doublet peak at 8.63 ppm. This peak is highly shifted because the proton is connected to an unsaturated carbon atom next to a highly electronegative nitrogen atom within the aromatic system. Finally, the NH of the hydrazine group shows a singlet peak at a chemical shift of 10.56 ppm. Thus, the  $^1\text{H-NMR}$  data are summarized in **Table 5**.

**Table 5.** The  $^1\text{H-}^{13}\text{C}$  NMR spectra for the L and the chemical shift in ppm.

Compound	$^1\text{H-NMR}$	$^{13}\text{C-NMR}$
L <sub>2</sub>	$\delta = 10.56$ ppm (S, 2H, 2NH), 8.63 ppm (dd, 2H, 2Ar-H next to N), 7.94 ppm (S, 2H, 2HC = N), 7.80-7.77 ppm (m, 4H, 4Ar-H), 7.51 ppm (m, 2H, 2Ar-H), 3.07 ppm (S, 2H, CH <sub>2</sub> ).	$\delta$ (ppm) = 167.11, 153.14, 148.11, 142.40, 137.61, 123.01, 119.09, 47.90.

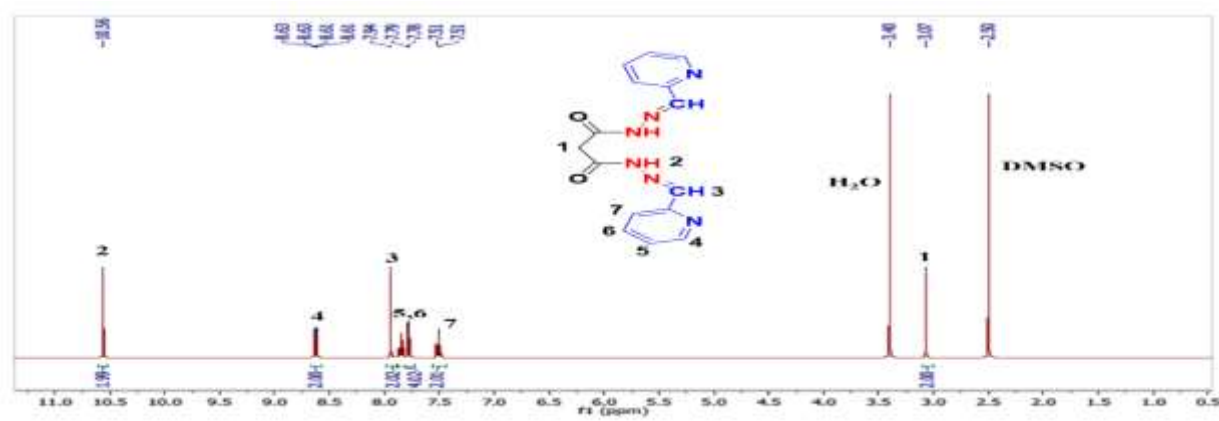


**Figure 7.** The  $^1\text{H-NMR}$  of ligand L<sub>2</sub>.

### 3.4 Carbon nuclear magnetic resonance spectroscopy ( $^{13}\text{C-NMR}$ )

Chemical shifts corresponding to all carbons of the ligand (DMSO-d<sub>6</sub>) are identified in a  $^{13}\text{C-NMR}$  spectrum, thus confirming their chemical structure. The chemical structure of the synthesized ligand, which has eight distinct carbon atom environments, is confirmed by the  $^{13}\text{C-NMR}$  spectroscopy, which revealed eight distinct peaks at corresponding chemical shifts.

**Figure 8** illustrates this chemical structure. The spectrum shows a peak at a chemical shift of 47.90 ppm, which belongs to the aliphatic CH<sub>2</sub> carbon atom. This peak has shifted to a higher chemical shift because it is next to two carbonyl groups, which cause the de-shielding of electrons around the corresponding carbon atom. On the other hand, the carbon atom of the carbonyl group (C=O) shows a peak at a chemical shift of 167.11 ppm. It is highly shifted because it is an unsaturated carbon atom next to oxygen. In our supposition, the five carbon atoms of the heteroaromatic unit show three peaks at 119.09, 123.01, and 137.61 ppm, and two carbons were shifted to a higher chemical shift, showing two peaks at 148.11 and 153.14 ppm. These peaks are highly shifted because they are an unsaturated carbon atom next to a highly electronegative nitrogen atom within the aromatic system. Finally, the carbon atom of the



azomethine group (HC=N) shows a peak at a chemical shift of 148.11 ppm. Thus, the  $^{13}\text{C}$ -NMR data are summarized in **Table 5**.

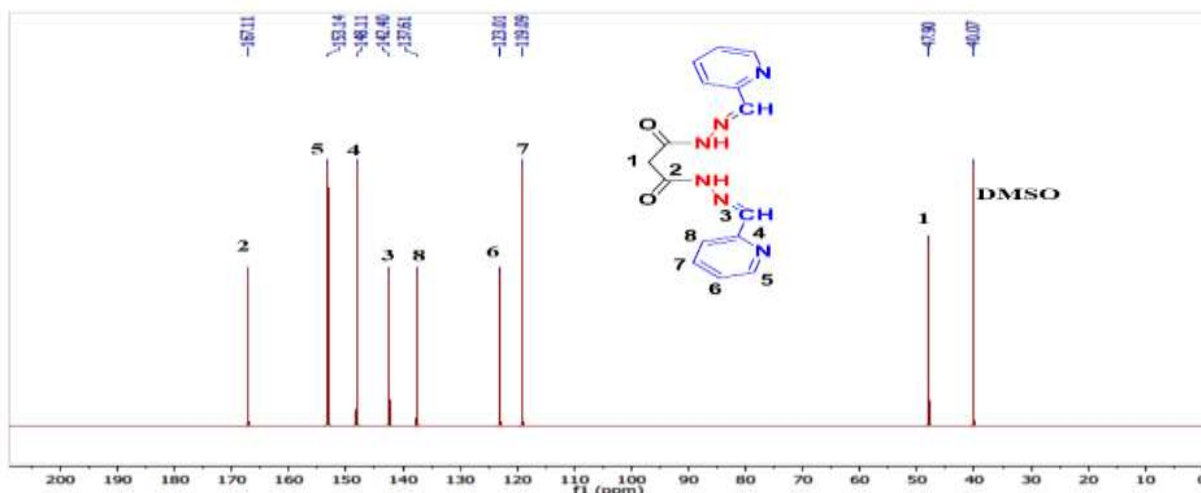


**Figure 8.** The  $^{13}\text{C}$ -NMR of ligand ( $L_2$ ).

### 3.5 Characterization of Schiff bases ligand by mass spectroscopy

Utilizing the mass spectrum method, one may ascertain the fragmentation that pertains to the compounds being studied as well as the molecular weight of the synthesized compounds. In **Figure 9**, the mass spectra of the prepared Schiff base ligand were consistent with the proposed structural formula  $\text{C}_{15}\text{H}_{14}\text{N}_6\text{O}_2$ . The molecular ion peak was found at  $m/e$  310, confirming their formula weight for ligand, which matches the estimated  $m^+$  value (310.32). Further unique peaks that were visible in the ligand mass spectra were the outcome of  $L_2$  further fragmentation.

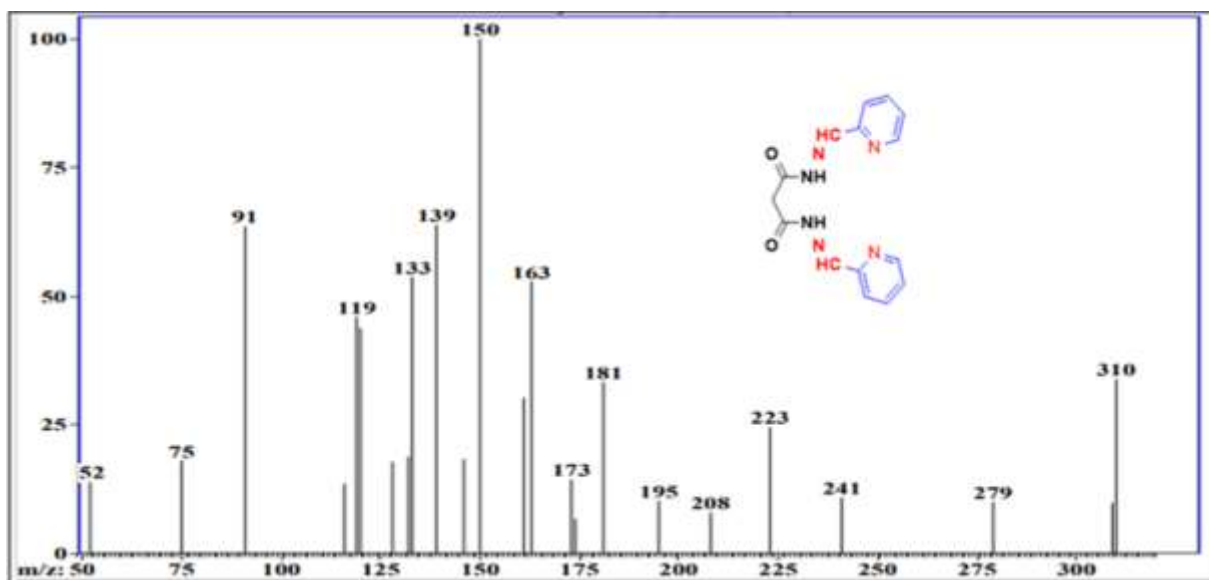


**Figure 9.** Mass spectrum of ligand.

### 3.6 Microbiological investigations

*In vitro*, the antibacterial activity of the ligands and their corresponding complexes was tested against Gram-negative (*Staph* and *Escherichia coli*) and Gram-positive (*Bacillus* and *Pseudomonas aeruginosa*) bacteria. The prepared compounds were highly effective. The synthesized ligands and their complexes were biologically active, as shown in **Table 6**.

The data obtained manifest that some of these compounds exhibited suitable activities against the tested organisms. Among the ligands and complexes, L<sub>2</sub> showed the highest activity against all bacterial species. In contrast, its complex [L<sub>2</sub>Co] showed maximum activity against Bacillus, and the L<sub>2</sub>Mn complex showed maximum activity against pseudomonas among the tested bacteria. **Table 6** and **Figures 10, 11** show the antibacterial activities of ligands and their corresponding complexes. The synthesized ligands and their II complexes were also subjected to antifungal activity against fungal strains (*Candida*). The antifungal activity results have shown that L<sub>2</sub> possessed and complexed the highest activity against *Candida* [25-30].

**Table 6.** Anti-bacterial activity of Schiff base L<sub>2</sub> and its complexes.

Compounds	<i>Staphylococcus aureus</i>	<i>E.Coli</i>	<i>Pseudomonas</i>	<i>Bacilla</i>	<i>Candida</i>
L <sub>2</sub>	14	17	17	17	16
Co <sup>+2</sup>	15	16	16	19	16
Mn <sup>+2</sup>	16	16	18	16	18

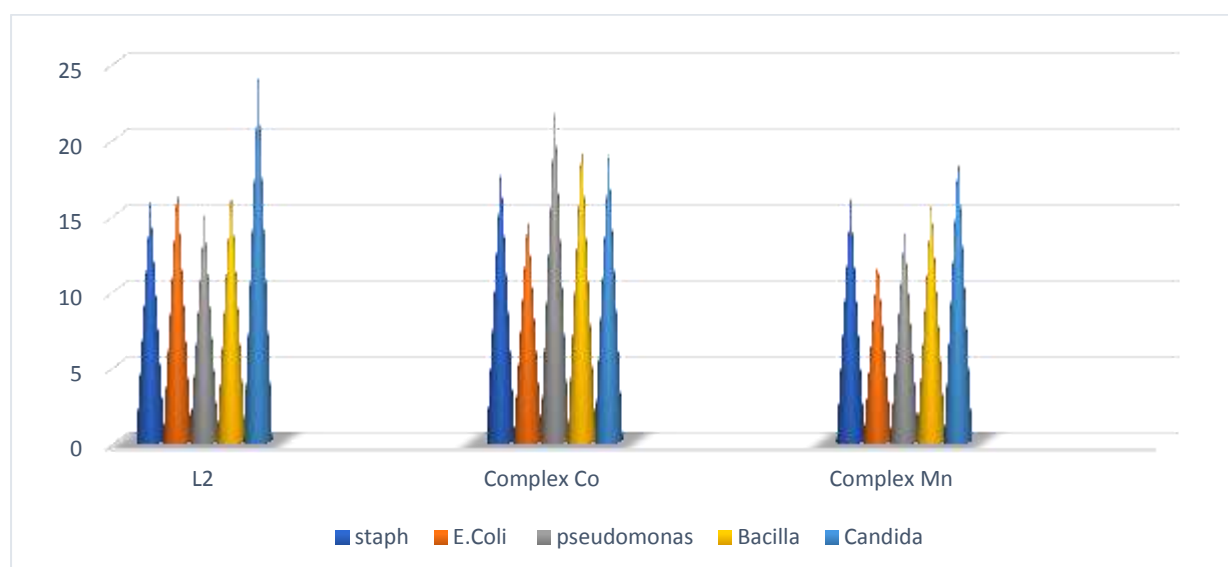


**Figure 10.** Anti-bacterial activity of Schiff base L<sub>2</sub> and its complexes.

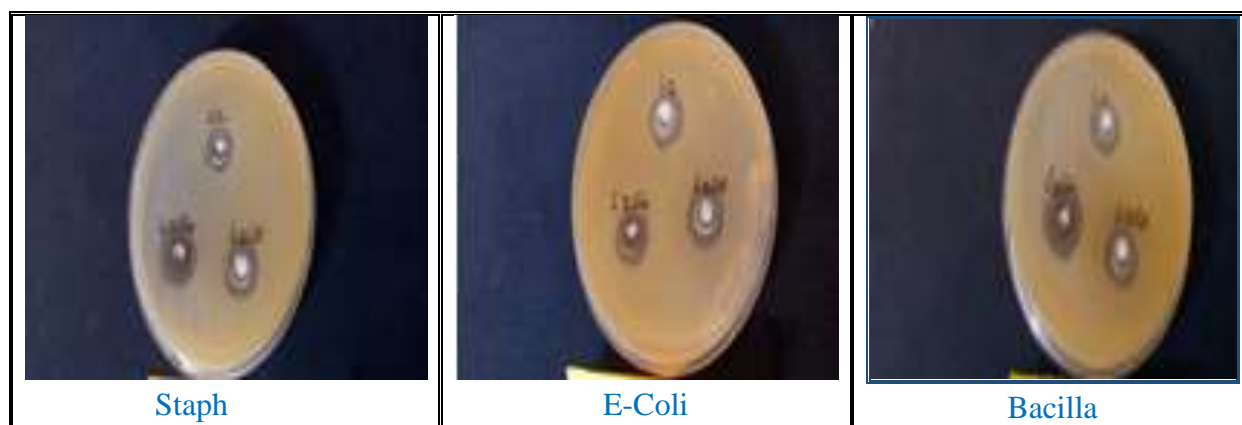


**Figure 11.** Biological activity of Schiff base L<sub>2</sub> and its complexes.

#### 4. Conclusion

The generated Schiff base complex operated as a tetradentate ligand, connecting to the metal ion via the nitrogen of pyridine and the nitrogen of azomethine, according to all of the investigation's spectrum data. Additionally, the analytical data demonstrated that all of the complexes that were generated had an M:L ratio of 1:1, which is compatible with a mononuclear structure. The spectrum and elemental analysis results, together with the complexes' magnetic moment and molar conductivity in DMF solution, demonstrated that every complex was an electrolyte with an octahedral structure. The biological activity of all the complexes is against two types of bacteria and fungi. *Escherichia coli*, *pseudomonas*, *Staphylococcus aureus*, *Bacilli*, and *Candida* were studied, and they gave good results in inhibition. It was suggested that the structure of the Schiff base complexes for L<sub>2</sub> is based on the characterization results, as shown in **Figure 12**.

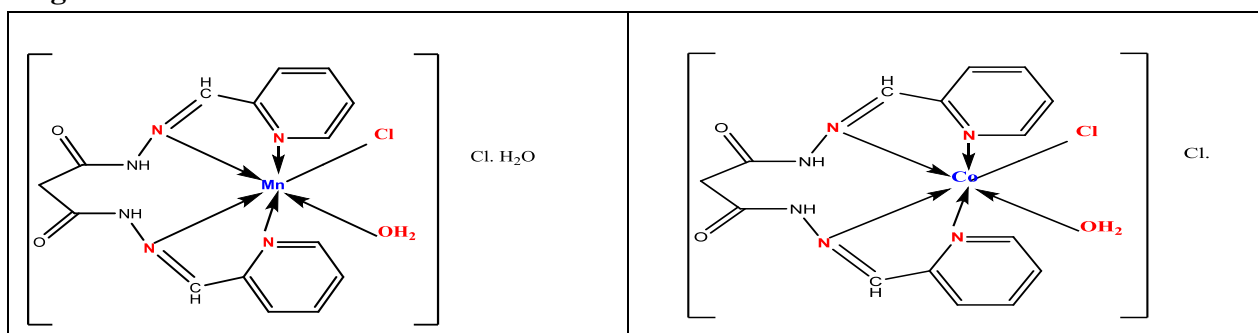


**Figure 12.** The proposed structure of Schiff base L<sub>2</sub> complexes.

#### Acknowledgment

The authors like to thank all who assisted in accomplishing this research.

#### Conflict of Interest

The authors confirm that all the figures and tables in the manuscript are to them. Besides, the statistics and images, which are not ours, have been permitted for republication and are attached to the manuscript.

#### Funding

There is no financial support.

#### Ethical Clearance

This work has been approved by the Institutional Scientific Committee at the University of Baghdad/ College of Sciences for Women.

#### References

1. de Oliveira Carneiro Brum, J.; França, T.C.; LaPlante, S.R.; Villar, J.D. Synthesis and biological activity of hydrazones and derivatives: A review. *Mini reviews in Med Chem* **2020**, *20*(5), 342-368. <https://doi.org/10.2174/1389557519666191014142448>.
2. Tazin, N.; Ragole, V.D.; Wankhede, D.S. Facile one pot synthesis of tetraamide macrocyclic complexes using malonyldihydrazide and p-nitrobenzaldehyde at room temperature. *Inorg Nano-Met Chem* **2019**, *49*(9), 291-296. <https://doi.org/10.1080/24701556.2019.1661449>.

3. Yang, Y.; Guo, L.; Ge, X.; Tian, Z.; Gong, Y.; Zheng, H.; Du, Q.; Zheng, X.; Liu, Z. Novel lysosome-targeted cyclometalated Iridium (III) anticancer complexes containing imine-N-heterocyclic carbene ligands: synthesis, spectroscopic properties and biological activity. *Dyes Pigm.* **2019**, *1(161)*, 119-129. <https://doi.org/10.1016/j.dyepig.2018.09.044>.
4. Muthuppalani, M.; Al Otaibi, A.; Balasubramaniyan, S.; Manikandan, S.; Manimaran, P.; Mathubala, G.; Manikandan, A.; Kamal, T.; Khan, A.; Marwani, H.M.; Alamry, K.A. An in-vitro anti-inflammatory and anti-microbial essential on Ni (II), Cd (II) mixed ligand complexes by using 2, 4-dinitrophenyl hydrazine and dimethylglyoxime. *J King Saud Univ Sci* **2022**, *34(5)*,102-114. <https://doi.org/10.1016/j.jksus.2022.102114>.
5. Verma, G.; Marella, A.; Shaquiquzzaman, M.; Akhtar, M.; Rahmat, A.M.; Mumtaz, A.M. A review exploring biological activities of hydrazones. *J Pharm Bioallied Sci* **2014**, *6(2)*,69-80. <https://doi:10.4103/0975-7406.129170>.
6. Kratky, M.; Stepankova, S.; Brablkova, M.; Svrckova, K.; Svarcová, M.; Vinsova, J. Novel iodinated hydrazide-hydrazones and their analogues as acetyl- and butyrylcholinesterase inhibitors. *Current Topics in Medicinal Chemistry* **2020**, *20(23)*,2106-2117. <https://doi.org/10.2174/1568026620666200819155503>.
7. Sanad, S.M.; Mekky, A.E. Synthesis, cytotoxicity and in vitro antibacterial screening of novel hydrazones bearing thienopyridine moiety as potent COX-2 inhibitors. *JICS* **2020**, *17(2)*, 3299-3315. <http://dx.doi.org/10.1007/s13738-020-01987-y>.
8. Bredihhin, A.; Groth, U.M.; Maeorg, U. Efficient methodology for selective alkylation of hydrazine derivatives. *Org Lett* **2007**, *9(6)*,1097-1099. <https://doi: 10.1021/ol070026w>.
9. Tsubrik, O.; Sillard, R.; Maeorg, U. Excellent regioselectivity is observed in the addition of diverse organometallic nucleophiles to unsymmetrical azo compounds. Primary/ secondary/tertiary alkyl, aryl and heteroaryl substituents were introduced this way in high yields. *Synth* **2006**, *5*,843-846. <https://doi:10.1055/s-2006-926331>.
10. Shaalan, N.; Mahdi, S. Synthesis, characterization and biological activity study of some new metal complexes with Schiff's bases derived from [O-Vanillin] With [2-Amino-5-(2-Hydroxy-Phenyl)-1,3,4-Thiadiazole]. *Egypt J Chem* **2021**, *64(8)*,4059-4067. <https://dx.doi.org/10.21608/ejchem.2021.66235.3432>.
11. Oguntoye, O. S.; Hamid, A.A.; Iloka, G.S.; Bodede, S.O.; Owalude, S.O.; Tella, A.C. Synthesis and spectroscopic analysis of Schiff bases of imesatin and isatin derivatives. *JASEM* **2016**, *20(3)*, 653-657. <https://doi:10.4314/jasem.v20i3.20>.
12. Hussein, K.A.; Shaalan, N. Synthesis, spectroscopy and biological activities studies for new complexes of some lanthanide metals with Schiff's bases derived from dimedone with 4-aminoantipyrine. *Chem Methodol* **2021**, *11*,103-113. <https://dx.doi.org/10.22034/chemm.2022.2.3>.
13. El-Saied, F.A.; Shakhofa, M.M.; Abdou, S.; Abd-Elzaher, M.M.; Morsy, N. Coordination versatility of N<sub>2</sub>O<sub>4</sub> polydentate hydrazone ligand in Zn (II), Cu (II), Ni (II), Co (II), Mn (II) and Pd (II) complexes and antimicrobial evaluation. *Beni-Suef Univ J Basic Appl Sci* **2017**, *6(4)*,310-320. <https://doi.org/10.1016/j.bjbas.2017.09.005>.
14. Al-Hamdani, A.A.; Shaalan, N.; Bakir, S.R.; Mohammed, M.S. Preparation, spectral characterization, structural study, and evaluation of antibacterial activity of Schiff base complexes for VOII, CrIII, MnII, ZnII, CdII and CeIII. *Baghdad Sci J* **2015**, *12(2)*,350-361. <https://bsj.uobaghdad.edu.iq/index.php/BSJ/article/view/2076>.
15. Shaalan, N.; Khalaf, W.M.; Mahdi, S. Preparation and characterization of new tetra-dentate N<sub>2</sub>O<sub>2</sub> Schiff base with some of metal ions complexes. *Indones J Chem* **2022**, *22(1)*,62-71. <https://doi.org/10.22146/ijc.66118>.
16. Echekwube, H.O.; Ukoha, P.O.; Ujam, O.T.; Nwuche, Ch.O.; Asegbeloyin, J.N.; Ibezim, A. Synthesis and in silico investigation of Schiff base derivatives of 1H-indole-2,3-diones and their Co(II) and

- Ni(II) complexes as antimicrobial agents. *Braz J Biol Sci* **2019**, *6(12)*,63-85. <https://doi.org/10.21472/bjbs.061207>.
17. Hussein, K.A.; Mahdi, S.; Shaalan, N. Synthesis, spectroscopy of new lanthanide complexes with Schiff base derived from (4-antipyrinecarboxaldehyde with ethylene di-amine) and study the bioactivity. *Baghdad Sci J* **2023**, *20(2)*,305-318. <http://dx.doi.org/10.21123/bsj.2022.7088>.
  18. Akcan Kardaş, T.; Avcı Özbek, H.; Akgül, Y.; Demirhan, F. Synthesis, structure, and electrochemical properties of N, N'-bis (ferrocenylmethylene) ethylenediamine Schiff base and its metal complexes. *Inorg Nano-Met Chem* **2017**, *47(10)*,1475-1479. <https://doi.org/10.1080/24701556.2017.1357586>.
  19. Rajakkani, P.; Alagarraj, A.; Thangavelu, S.A.Tetraaza macrocyclic Schiff base metal complexes bearing pendant groups: Synthesis, characterization and bioactivity studies. *Inorg. Chem. Commun.* **2021**,*134*,108989. <https://doi.org/10.1016/j.inoche.2021.108989>.
  20. Orojloo, M.; Amani S. Colorimetric detection of pollutant trivalent cations and HSO<sub>4</sub><sup>-</sup> in aqueous media using a new Schiff-base probe: An experimental and DFT studies. *PAHS* **2021**, *41(1)*,33-46. <https://doi.org/10.1080/10406638.2019.1567561>.
  21. Najeeb, D.A.; Ahmed, A.; Yusop, M.R. Synthesis, characterization and theoretical study of 1, 2 (2, 2-dihydroxy benzelidenamine) phenyl complexes. *ANJS* **2017**, *20(3)*,12-17. <https://doi:10.22401/JUNS.20.3.03>.
  22. Jawad, W.A.; Balakit, A.A.; Al-Jibouri, M.N. Synthesis, characterization and antibacterial activity study of cobalt (II), nickel (II), copper (II), palladium (II), cadmium (II) and platinum (IV) complexes with 4-Amino-5-(3, 4, 5-trimethoxyphenyl)-4 H-1, 2, 4-triazole-3-thione. *Indones J Chem* **2021**, *21(6)*,1514-1525. <https://doi.org/10.22146/ijc.67021>.
  23. Ayoub, M.A.; Abd-Elnasser, E.H.; Ahmed, M.A.; Rizk, M.G. Some new metal (II) complexes based on bis-Schiff base ligand derived from 2-acetylethiophine and 2, 6-diaminopyridine: Syntheses, structural investigation, thermal, fluorescence and catalytic activity studies. *Journal of Molecular Structure* **2018**, *1163*,379-387. <https://doi.org/10.1016/j.molstruc.2018.03.006>.
  24. Zulfikaroğlu, A.; Ataol, Ç.Y.; Çelikoğlu, E.; Çelikoğlu, U.; İdil, Ö. New Cu (II), Co (III) and Ni (II) metal complexes based on ONO donor tridentate hydrazone: Synthesis, structural characterization, and investigation of some biological properties. *J Mol Struct* **2020**, *1199(31)*, 127012. <http://dx.doi.org/10.1016/j.molstruc.2019.127012>.
  25. Shaalan, N. Preparation and spectroscopic study, biological and thermodynamic activity of new complexes of some metal ions with 2-[5-(2-hydroxy-phenyl)-4, 3, 1-thiadiazol-2-ylimino]-methyl-naphthalene-1-ol. *Baghdad Sci J* **2022**, *19(4)*,829-837.<https://doi.org/10.21123/bsj.2022.19.4.0829>.
  26. Hachim, L.S.; Khalaf, K.J.; Aljoofy, I.K. Thrombolytic activity of purified staphylokinase produced from clinical isolates. *Int J Drug Deliv Technol* **2020**, *10(4)*,571-576.
  27. Denamur, E.; Clermont, O.; Bonacorsi, S.; Gordon, D. The population genetics of pathogenic *Escherichia coli*.*Nat. Rev.Microbiol.* **2021**,*19(1)*,37-54.<https://doi.org/10.1038/s41579-020-0416-x>.
  28. Joseph, L.; Merciecca, T.; Forestier, C.; Balestrino, D.; Miquel, S. From klebsiella pneumoniae colonization to dissemination: An overview of studies implementing murine models. *MDPI* **2021**, *9(6)*,1282. <https://doi.org/10.3390/microorganisms9061282>.
  29. Mali, S.N.; Thorat, B.R.; Gupta, D.R.; Pandey, A. Mini-review of the importance of hydrazides and their derivatives—synthesis and biological activity. *Engineering Proceedings* **2021**, *11(1)*,21. <https://doi.org/10.3390/ASEC2021-11157>.
  30. Ansari, A.; Tauro, S.; Asirvatham, S. A Systematic review on synthetic and antimicrobial bioactivity of the multifaceted hydrazone derivatives. *Mini-Reviews in Organic Chemistry* **2022**, *19(4)*,522-543. <https://doi.org/10.2174/1570193X18666210920141351>.